Structural and biological mimicry of protein surface recognition by α/β-peptide foldamers

W. Seth Horne[a], Lisa M. Johnson[a], Thomas J. Ketas[b], Per Johan Klasse[b], Min Lu[c], John P. Moore[b], and Samuel H. Gellman[a,1]

[a]Department of Chemistry, University of Wisconsin, 1101 University Avenue, Madison, WI 53706; [b]Department of Microbiology and Immunology, Weill Medical College of Cornell University, New York, NY 10021; and [c]Department of Biochemistry, Weill Medical College of Cornell University, New York, NY 10021

Edited by David Baker, University of Washington, Seattle, WA, and approved July 2, 2009 (received for review March 10, 2009)

Unnatural oligomers that can mimic protein surfaces offer a potentially useful strategy for blocking biomedically important protein-protein interactions. Here we evaluate an approach based on combining α- and β-amino acid residues in the context of a polypeptide sequence from the HIV protein gp41, which represents an excellent testbed because of the wealth of available structural and biological information. We show that α/β-peptides can mimic structural and functional properties of a critical gp41 subunit. Physical studies in solution, crystallographic data, and results from cell-fusion and virus-infectivity assays collectively indicate that the gp41-mimetic α/β-peptides effectively block HIV-cell fusion via a mechanism comparable to that of gp41-derived α-peptides. An optimized α/β-peptide is far less susceptible to proteolytic degradation than is an analogous α-peptide. Our findings show how a two-stage design approach, in which sequence-based $\alpha \rightarrow \beta$ replacements are followed by site-specific backbone rigidification, can lead to physical and biological mimicry of a natural biorecognition process.

alpha/beta-peptides | HIV | protein folding | protein–protein interactions

Identification of strategies for interference with specific biopolymer recognition processes constitutes a fundamental challenge. Protein-protein associations are often resistant to inhibition by small molecules because the contact surfaces on the natural partners are large (1). Current clinical approaches to inhibiting protein-protein interactions that underlie viral infection or aberrant signaling at the cell surface are based on the use of medium-length peptides or proteins (2). It would be valuable to identify alternative sources of antagonists for this type of protein recognition event. Here we show that peptide-like oligomers with unnatural backbones can function as potent antiviral agents by blocking a key protein–protein interaction. The design strategy we employ may prove general for α-helix mimicry.

The HIV membrane protein gp41 mediates viral envelope-host cell membrane fusion, an essential step in the viral infection cycle. During HIV cell entry, the N-terminal fusion segment of trimeric gp41 inserts into the host cell membrane (3). A profound structural rearrangement of gp41 ensues, driven by formation of an antiparallel six-helix bundle (4–6), which leads to juxtaposition of the viral and host cell membranes. The prehairpin fusion intermediate is composed of three copies of gp41 in an extended conformation. The so-called "class I" fusion mechanism used by HIV is common to a variety of enveloped viruses, including those responsible for influenza, Ebola, and SARS (7, 8). A number of α-peptides based on sequences from the gp41 N-terminal heptad repeat (NHR) domain or C-heptad repeat (CHR) domain (e.g., Fig. 1*B*, **1** and **2**) have been investigated as anti-HIV agents (9, 10). These compounds are thought to act by binding to a gp41 prehairpin intermediate, thereby preventing six-helix bundle formation and subsequent virus-cell fusion. The drug enfuvirtide (**T-20**), a 36-residue α-peptide derived from the CHR region, is used clinically as an anti-HIV agent (9, 10). However, enfuvirtide is rapidly degraded in vivo and must be administered twice daily in large doses; development of potent fusion inhibitors that resist physiological degradation remains a challenging goal (11–17). The only non-protein gp41 mimics reported to date that show IC_{50} values <1 μM in cell-based assays are multivalent species displaying two or three copes of a phage-derived D-peptide (16).

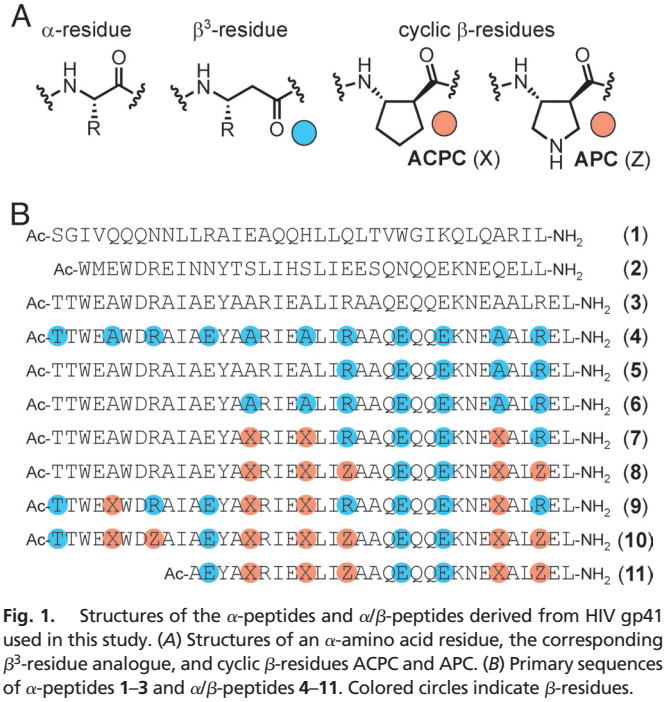

Fig. 1. Structures of the α-peptides and α/β-peptides derived from HIV gp41 used in this study. (*A*) Structures of an α-amino acid residue, the corresponding β^3-residue analogue, and cyclic β-residues ACPC and APC. (*B*) Primary sequences of α-peptides **1**–**3** and α/β-peptides **4**–**11**. Colored circles indicate β-residues.

Oligomers that display folding properties akin to those of proteins and nucleic acids but bear unnatural backbones have been the subjects of extensive study (18–23). Efforts to create and understand these molecules, often termed "foldamers," are motivated by etiological as well as practical considerations. We have recently begun to explore mimicry of the conformational propensities and function encoded in natural polypeptide sequences by oligomers in which subsets of α-amino acid residues are replaced with β^3-residues bearing the same side chain (Fig. 1*A*). Preliminary findings indicated that this sequence-based design strategy generates α/β-peptides that can form protein-like quaternary assemblies or mimic

Author contributions: W.S.H., L.M.J., P.J.K., M.L., J.P.M., and S.H.G. designed research; W.S.H., L.M.J., T.J.K., and M.L. performed research; W.S.H., L.M.J., P.J.K., M.L., J.P.M., and S.H.G. analyzed data; and W.S.H. and S.H.G. wrote the paper.

The authors declare no conflict of interest.

This article is a PNAS Direct Submission.

Data deposition: The atomic coordinates have been deposited in the Protein Data Bank, www.pdb.org (PDB ID codes 3F4Y, 3F4Z, 3F50, and 3G7A).

[1]To whom correspondence should be addressed. E-mail: gellman@chem.wisc.edu.

This article contains supporting information online at www.pnas.org/cgi/content/full/0902663106/DCSupplemental.

Table 1. Summary of physical and functional data obtained for gp41 CHR analogues 3–11

	gp41–5 binding affinity by FP*	NHR + CHR stability by CD†	Stability to Proteinase K‡	Cell-cell fusion inhibition§	Inhibition of HIV-1 infectivity, IC_{50}, nM¶			
					X4 strains		R5 strains	
Oligomer	K_i, nM	$T_{m,app}$, °C	$t_{1/2}$, min	IC_{50}, nM	NL4–3	HC4	CC 1/85	DJ258
3	< 0.2	77	0.7	9 ± 3	5 ± 0.6	27 ± 4	140 ± 20	58 ± 6
4	3,800	-‖	14	390 ± 40	700 ± 60	590 ± 100	1300 ± 100	960 ± 200
5	< 0.2	67		7 ± 2	10 ± 2	55 ± 8	270 ± 20	280 ± 90
6	15							
7	0.4							
8	0.3	65						
9	83							
10	9	55	200	5 ± 2	28 ± 3	59 ± 10	180 ± 30	110 ± 40
11	> 10,000							
T-20					700 ± 100	250 ± 20	1400 ± 400	330 ± 60

*Dissociation constant (K_i) for binding to the protein gp41–5 as determined by competition FP experiments.

†Apparent melting temperature ($T_{m,app}$) for the thermal unfolding transition observed by CD at 222 nm for a 1:1 mixture of NHR α-peptide **1** and the indicated CHR analogue at 20 μM total peptide concentration in PBS.

‡Half-life ($t_{1/2}$) of a 20 μM solution of peptide in TBS in the presence of 10 μg/mL proteinase K.

§Values are the means ± SEM of IC_{50} values obtained in three independent experiments. The envelope protein expressed was of the HxB2 clone, derived from the T-cell-line-adapted isolate IIIB of clade B.

¶Values are the means ± SEM of IC_{50} values obtained in three independent experiments.

‖The temperature-dependent CD for the **1** + **4** mixture was not significantly different from that calculated based on the average of the temperature-dependent CD spectra of **1** alone and **4** alone.

short α-helical domains involved in apoptotic signaling (24–26). The gp41 protein represents an attractive target for exploratory studies related to sequence-based backbone modification because of the extensive structural data available for this system and the prospect of evaluating the functional consequences of backbone alterations in biological assays. This target stands out relative to others that have been used to explore unnatural oligomer designs because effective inhibition appears to require mimicry of a long α-helix (~10 turns). Here, we show that sequence-based backbone modification of gp41-derived α-peptides can generate α/β-peptides that mimic key structural and functional properties of HIV gp41 and display significant resistance to proteolytic degradation.

Results

First Generation α/β-Peptide gp41 Mimic Designs and in Vitro Protein Binding Assays. We selected a recently reported gp41 CHR-derived α-peptide, **3** (27), as the starting point for α→β modification (Fig. 1). α-Peptide **3**, also known as T-2635, is 50% mutated as compared with the wild-type gp41 CHR domain and contains a combination of Xxx→Ala substitutions and engineered $i \rightarrow i+4$ salt bridges that enhance α-helical propensity (27). α-Peptide **3** represents one of the most successful examples reported to date of improving the antiviral efficacy of gp41 CHR α-peptides via modification of the α-amino acid sequence. We began with the side chain sequence optimized in **3** and explored the orthogonal variable of backbone composition in the form of α→β residue substitution [a method we term "sequence-based design" (24–26)]. In α/β-peptide **4**, a subset of the α-residues in **3** has been replaced by corresponding β^3-residues (Fig. 1*A*). Thus, α/β-peptide **4** has the sequence of side chains found in **3** displayed on an unnatural backbone. The β^3-residues of **4** are incorporated in an ααβααααβ pattern, which generates a stripe of β-residues that runs along one side of the helix (24). Our design places the β-stripe in **4** distal along the helix circumference to the molecular surface that packs against the gp41 NHR domain trimer in the six-helix bundle.

We used a previously reported competition fluorescence polarization (FP) assay (15) to compare **3** and **4**. The assay measures displacement of a fluorescently labeled CHR α-peptide from an engineered five-helix bundle protein, gp41–5, which contains three NHR segments and two CHR segments. Affinity for the gp41–5 protein construct is expected to correlate with the ability of CHR-mimetic agents to bind to the gp41 prehairpin intermediate formed just before HIV-cell fusion (15). As expected, α-peptide **3** binds very tightly to gp41–5 (K_i < 0.2 nM; Table 1). The analogous α/β-peptide **4**, however, displays only weak affinity for gp41–5, >10,000-fold lower than that of **3**. The modest potency of α/β-peptide **4** in this protein-based assay is similar to that displayed by many small molecules and peptidomimetics in comparable experiments (11–17).

In an effort to understand the dramatic differences in binding between **3** and **4**, we prepared and characterized chimeric α/β-peptides **5** and **6**. Both **5** and **6** contain a pure α segment at the N terminus and an α/β segment at the C terminus (28); these oligomers are chimeras of α-peptide **3** and α/β-peptide **4**. α/β-Peptide **5** displays very high affinity for gp41–5, indistinguishable from that of α-peptide **3**; however, extending the α/β segment toward the N terminus (as in **6**) causes a significant loss of affinity. The sensitivity of the N-terminal segment to α→β^3 modification is consistent with data showing that side chains in this region, especially those corresponding to Trp_3, Trp_6, and Ile_{10} in **3**, play a crucial role in CHR binding to the NHR trimer (29).

Second Generation α/β-Peptide gp41 Mimics with Rigidified Backbones. α/β-Peptides **5** and **6** represent an improvement in gp41 mimicry relative to 4 (vide supra), but it would be desirable to place β-residues throughout an α/β-peptide sequence to maximize resistance to proteolysis (30–32). Each α→β^3 replacement, however, adds a flexible bond to the backbone, which should increase the conformational entropy penalty associated with helix formation (26, 33, 34). The greater conformational entropy of the unfolded state of **4** relative to **3**, arising from eleven α→β^3 replacements, may account for the large difference in binding affinity for gp41–5 between these two oligomers. β-Residues provide an avenue for conformational preorganization that is made uniquely possible by their chemical structure. Incorporation of cyclic β-residues (e.g., ACPC and APC; Fig. 1*A*) can constrain the C_α-C_β backbone torsion and thereby enhance folding propensity without disrupting backbone amide hydrogen bonding (35–37).

We probed the impact of conformational preorganization in the context of gp41 mimicry by replacing a subset of β^3-residues with

cyclic analogues. The first comparison involved α/β-peptide **7**, the analogue of **6**, in which the three β^3-hAla residues are replaced by ACPC (Fig. 1*A*). Both β^3-hAla and ACPC are nonpolar, and this similarity was expected to maintain the physical properties that emerge from side chain sequence. The >30-fold higher affinity for gp41–5 displayed by **7** relative to **6** supports our hypothesis that residue-based rigidification is a useful complement to sequence-based design for development of peptide-mimetic foldamers. Replacement of two β^3-hArg residues in oligomer **7** with APC, a heterocyclic analogue of ACPC, leads to α/β-peptide **8**, which showed a very high affinity for gp41–5. APC_{36} of **8** is in a region that does not engage the NHR region contained in gp41–5; this observation may explain the similar K_i values of **7** and **8**. Additional evidence of the favorable contribution of cyclic β-residues comes from comparison of oligomers **4**, **9**, and **10**, each of which has β-residues throughout the sequence. α/β-Peptide **9** was generated from **4** by four β^3-hAla→ACPC replacements, which leads to a >45-fold improvement in K_i. Replacement of the three β^3-hArg residues of **9** with APC, to generate **10**, improves K_i by a further ~10-fold. Relative to completely flexible α/β-peptide **4**, rigidified analogue **10** (K_i = 9 nM) shows ~380-fold enhanced binding to gp41–5.

Physical Characterization of Six-Helix Bundle Formation in Solution. We investigated the interactions of CHR α-peptide **3** and α/β-peptide analogs **4**, **5**, **8**, and **10** with gp41 NHR peptide **1** by circular dichroism (CD) spectroscopy. When mixed with gp41 CHR α-peptides, NHR-peptide **1** forms a six-helix bundle that is thought to represent the postfusion state adopted by gp41 in the course of viral entry (4). α-Peptide **3** showed significant helical content at 20 μM in PBS, consistent with previously published data (Fig. 2*A*) (27). α/β-Peptide **4** showed little helicity under similar conditions; however, analogue **10**, with seven β^3→cyclic-β substitutions, showed an intense CD minimum, consistent with a well-folded α/β-peptide helix (24). We compared the observed CD spectrum for each 1:1 mixture of NHR+CHR peptide (Fig. 2*B*, solid lines) to that calculated by averaging spectra for the corresponding individual oligomers (Fig. 2*B*, dashed lines). α/β-Peptides **5**, **8**, and **10**, which displayed high affinity for gp41–5 in the competition FP assay, each showed a significant degree of induced helicity when mixed with NHR α-peptide **1**, consistent with six-helix bundle formation. By contrast, α/β-peptide **4**, which has only modest affinity for gp41–5, showed essentially no interaction with **1**. The magnitude of the CD signatures among the well-folded mixtures is similar, but the ratio of intensities at 208 and 222 nm changes as a function of β-residue content. This trend is consistent with our previous studies on helical oligomers containing mixed α/β backbones (24, 26). The complexes formed by **1**+**3**, **1**+**5**, **1**+**8**, and **1**+**10** each showed highly cooperative thermal transitions (Fig. 2*C*). The trend in apparent T_m values ($T_{m,app}$) correlates with differences in affinity among **3**, **5**, **8**, and **10** for gp41–5 in the competition FP assay (Table 1); that is, stronger binding to gp41–5 correlates with more stable assembly with NHR peptide **1**.

Crystal Structures. We used X-ray crystallography to compare the heteromeric six-helix bundles formed by NHR α-peptide **1** with CHR α-peptide **3**, chimeric CHR α/β-peptide **8**, or CHR α/β-peptide **10** (Fig. 3, Table S1, and Fig. S1). Although the mutations to the native CHR sequence that lead to α-peptide **3** were not intended to modify the nature of its binding interactions with the gp41 NHR domain (27), we sought direct evidence that the six-helix bundle structure was unchanged relative to that formed by **1** and the native CHR sequence (4). We obtained a cocrystal of α-peptides **1** and **3** and solved the structure to 2.0 Å resolution. The resulting six-helix bundle (Fig. 3*A*) is essentially identical to that previously reported for **1**+**2** (4), which contains the native CHR sequence; the root mean square deviation (rmsd) is 0.73 Å for C_α atoms.

We obtained a crystal of the **1**+**10** complex and solved the structure to 2.8 Å resolution. α-Peptide **1** and α/β-peptide **10** combine to form a six-helix bundle that is similar to that formed by **1**+**3** (Fig. 3*A*). A crystal containing only α/β-peptide **10** was obtained as well. The structure of **10** alone (Fig. S2), solved to 2.1 Å resolution, revealed a parallel trimeric helix bundle with a hydrophobic core comprising the residues that engage the gp41 NHR trimer **1**+**10**. The self-assembly of α/β-peptide **10** in the crystalline state parallels the behavior previously observed for prototype α-peptide **3**, which was shown to self-assemble in solution (27).

The core NHR trimers in the structures of **1**+**10** and **1**+**3** are highly homologous (0.65 Å C_α rmsd for NHR residues 3–30). When the two bundles are aligned via the NHR trimer (Fig. 3*B*), the CHR helices track very closely in the C-terminal segment (0.84 Å C_α rmsd for residues 16–33), but diverge near the N terminus (4.2 Å C_α rmsd for residues 2–15). This divergence reflects a greater superhelical twist in α-peptide **3** relative to α/β-peptide **10**. The divergent

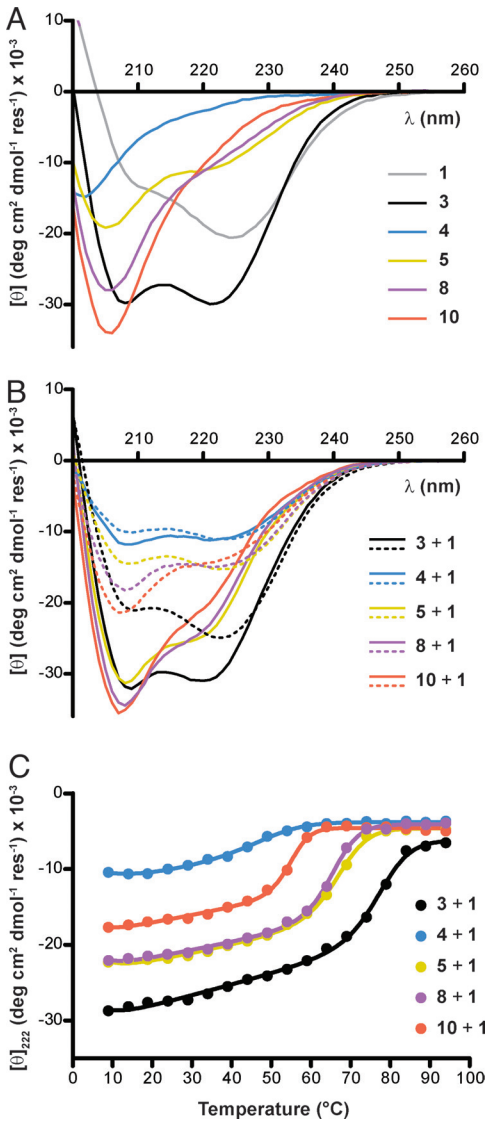

Fig. 2. Circular dichroism data for NHR peptide **1** and CHR peptides **3**, **4**, **5**, **8**, and **10**. (*A*) CD spectra of the individual oligomers at 20 μM concentration in PBS at 25 °C. (*B*) CD spectra of the indicated 1:1 mixtures at a total concentration of 20 μM in PBS at 25 °C (solid lines) along with the spectra calculated for 1:1 noninteracting mixtures from CD measurements on the individual components (dashed lines). (*C*) Temperature-dependent molar ellipticity at 222 nm for the indicated complexes at 20 μM concentration in PBS.

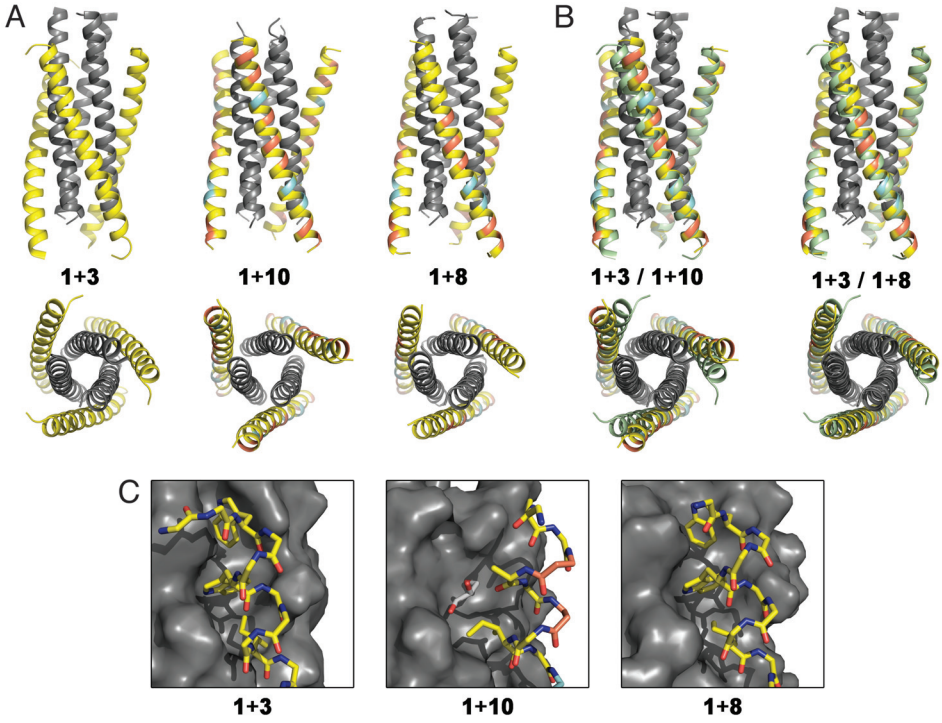

Fig. 3. Crystal structures of the six-helix bundles formed by NHR α-peptide **1** in complex with α-peptide **3**, α/β-peptide **10**, or chimeric α/β-peptide **8**. (*A*) Views from the side and looking down the superhelical axis of the indicated six-helix bundles. NHR helices are colored gray, CHR helices are colored by residue type (yellow for α, cyan for β^3, and red for cyclic β). (*B*) Overlay of the all α-peptide helix bundle formed **1**+**3** with that formed by **1**+**10** or **1**+**8**. The CHR helix from **1**+**3** is colored green; otherwise, coloring is the same as in *A*. In *A* and *B*, the structures viewed from the side are oriented with the CHR N terminus at the top of the page; the structures viewed down the superhelical axis are oriented with the CHR N terminus projecting out of the page. (*C*) Packing interactions of CHR residues Trp_3, Trp_6, and Ile_{10} (shown as sticks) against the NHR core trimer (shown as surface) in the structures of **1**+**3**, **1**+**10**, and **1**+**8**; in the structure of **1**+**10**, neither Trp_3 nor Trp_6 was resolved in electron density past C_β, and a molecule of glycerol (shown as sticks) was observed in the Trp_6 binding cavity. Coloring is the same as in *A*.

portion of the helix formed by **10** contains the two Trp residues that, in CHR α-peptides, are essential for stable six-helix bundle formation (Fig. 3*C*) (29). In the structure of **1**+**10**, the side chains of Trp_3 and Trp_5 were not resolved in electron density, suggesting a high degree of disorder. In addition, significant disorder was observed in the side chains of NHR residues Lys_{29} and Trp_{26}, which pack around CHR Trp_5 in the **1**+**3** complex.

Given the well-established role of the gp41 CHR domain Trp-Trp-Ile motif in six-helix bundle formation (29), the observation that the N-terminal segment of α/β-peptide **10** does not engage the NHR binding pocket in the crystal structure of the **1**+**10** complex is intriguing. Removal of the first 10 residues of α/β-peptide **10** leads to oligomer **11**, in which the Trp-Trp-Ile motif is not present. α/β-Peptide **11** showed no measurable affinity for gp41–5 ($K_i > 10$ μM), indicating that the N-terminal segment of **10** is essential for high-affinity binding to gp41–5 in solution.

Motivated by the differences between the CHR domain, N-terminal segments in the **1**+**3** complex and the **1**+**10** complex, we investigated the structure of NHR peptide **1** in complex with CHR α/β-peptide **8**, a chimera of α-peptide **3** and α/β-peptide **10**. We crystallized the **1**+**8** complex and solved the structure to 2.8 Å resolution. Relative to α/β-peptide **10**, chimeric α/β-peptide **8** tracks much more closely with the CHR helix (3) in the all α-peptide six-helix bundle formed by **1**+**3** (1.4 Å C_α rmsd for residues 2–33; Fig. 3 *A* and *B*). The side chains of the Trp-Trp-Ile motif in the N-terminal segment of **8** show the expected packing into the binding pocket on the NHR core trimer (Fig. 3*C*). Based on this result and the behavior of truncated α/β-peptide **11**, we suspect that the lack of direct contact between the N-terminal portion of **10** and the NHR trimer in the **1**+**10** complex is an artifact of crystal packing.

Antiviral Activity. We performed two sets of experiments to evaluate the activities of α-peptide **3** and α/β-peptides **4**, **5**, and **10** in a biological context. We first compared the oligomers in a cell-cell fusion assay based on expression of the *env* gene of the HIV-1 clone HxB2, an assay that is commonly used to model gp41-mediated HIV-cell fusion (38). The cell-cell fusion assay results (Table 1) showed that α/β-peptides **5** and **10** have IC_{50} values indistinguishable from that of α-peptide **3**, whereas α/β-peptide **4** is much less effective. We then evaluated **3**, **4**, **5**, and **10** for the ability to prevent HIV infection of the cell line TZM-bl (39). These studies used one T-cell-line-adapted strain and three primary isolates of HIV; two of the strains are X4-tropic, and the other two are R5-tropic. The infectivity assay results (Table 1 and Fig. S3) show similar biological potencies among **3**, **5**, and **10** for HIV-1 strains that use different coreceptors; this finding suggests the blocking of a necessary, shared step in entry through peptide interactions with conserved regions of gp41. It may be noted that there is imperfect correlation between K_i for binding to gp41–5 and IC_{50} values in cell-based assays among the compounds reported here. For example, the affinity of **10** for gp41–5 was >45-fold lower than that of **5**, yet IC_{50} values for **10** were sometimes lower than for **5**. There are several possible reasons for this discrepancy. Sequence differences between the CHR and NHR domains found in gp41–5 and those found in the viruses tested may lead to better correlation between gp41–5 binding affinity and antiviral activity against some strains relative to others. In addition, it has previously been suggested that the association rates for CHR peptides binding to gp41 are a better predictor of relative antiviral potencies than are equilibrium binding affinities (40). The rigidified backbone in **10** may alter its association rate with gp41 relative to that of **5**. Sensitivity to gp41-derived fusion inhibitors may be affected by many factors that differ among strains of virus, including the amount of Env incorporated into the virion, the strength of Env interactions with CD4 and with coreceptors, the kinetics and energetics of the fusion process, as well as amino acid variation in the binding site for inhibitory peptides. Overall, the antiviral assays results support our hypothesis that CHR-derived α/β-peptides effectively mimic gp41 in a complex biological milieu.

Proteolytic Susceptibility. An important motivation for the development of foldamer antagonists of protein–protein interactions is the prospect of diminishing sensitivity to proteolytic degradation. Rapid destruction in vivo represents a significant drawback to the clinical use of α-peptide drugs. We compared the susceptibilities of α-peptide **3** and α/β-peptides **4** and **10** toward degradation by proteinase K, a promiscuous serine protease. Under the assay

conditions, α-peptide **3** was completely degraded within minutes; mass spectrometry revealed hydrolysis of at least 10 different amide bonds in the sequence (Fig. S4). α/β-Peptide **4**, with exclusively $\alpha \rightarrow \beta^3$ substitution, showed 20-fold improvement in stability relative to prototype α-peptide **3**. Rigidified α/β-peptide **10** showed an even greater improvement in stability over α-peptide **3** (280-fold). The greater stability of α/β-peptide **10** relative to α/β-peptide **4** likely results from the greater helical propensity of **10**, as detected by CD. The small number of proteolysis products observed for α/β-peptide **10** supports previous observations that β-residues in mixed α/β backbones tend to protect neighboring amides from proteolytic cleavage (25, 31).

Discussion

Many proteins display surfaces that participate in highly selective interactions. Information flow mediated by protein–protein interactions is essential for normal biological function; such interactions can play key roles in disease as well. There is considerable motivation to identify strategies for inhibiting the formation of specific interprotein complexes. At the clinical level, the most successful approach involves the use of engineered proteins or protein fragments (2). Our motivating hypothesis is that recognition surfaces displayed by proteins can be mimicked with unnatural oligomers that adopt protein-like conformations and display protein-like side chains, and that such oligomers should function as inhibitors of protein–protein associations. We believe that natural protein sequences are logical starting points for the design of such oligomers. The data presented here provide strong support for these hypotheses.

Our results indicate that a long α-helical segment, the CHR region of HIV protein gp41, can be structurally and functionally mimicked by oligomers composed of α- and β-amino acid residues. A two-stage process was required to generate an α/β-peptide that manifests a favorable profile of properties, including strong association with the intended binding partner, potent inhibition of HIV infection in a cell-based assay, and resistance to proteolytic cleavage. The first design stage involves replacement of selected α-residues in a parent peptide sequence with homologous β-residues that retain the original side chains. The second design stage involves selective replacement of flexible β^3-residues with cyclically preorganized β-residues. These modifications are intended to remove deleterious backbone flexibility that is unavoidably introduced with the initial $\alpha \rightarrow \beta^3$ modifications (34).

The necessity of a two-stage approach for creation of an effective α/β-peptide mimic of the gp41 CHR segment is noteworthy in light of our previous findings in a different and inherently simpler protein recognition system. Mimicry of BH3 domains, short α-helical segments that mediate protein–protein interactions in the Bcl-2 protein family, required only the first stage of our design approach, simple $\alpha \rightarrow \beta^3$ substitution throughout the prototype sequence (25). By contrast, α/β-peptide **4**, which showed only modest affinity for gp41–5, was the most potent gp41 mimic we identified among a series of α/β-peptides designed by exploring alternative α/β^3 backbone patterns in the native gp41 CHR domain and related sequences (Fig. S5).

Ultimate success of foldamer-based strategies for functional protein mimicry will depend on developing an intimate understanding of folding propensities of unnatural backbones. Results from the present work suggest a set of subtle but important distinctions between pure α and mixed α/β backbones, as illustrated by comparison of the structural and functional data obtained for CHR α/β-peptides **10** and **8**. The crystal structure of the **1**+**10** complex supports our design hypothesis that gp41 CHR α/β-peptides engage the core NHR trimer via six-helix bundle formation, but the **1**+**10** structure also yields the unexpected observation that the Trp-Trp-Ile motif in the CHR N-terminal segment does not engage the NHR binding pocket. Replacement of the α/β segment in the N-terminal region of **10** with an α-peptide segment generates chimeric **8**, which, relative to **10**, shows a much higher affinity for gp41–5 and a backbone CHR helix conformation that is more similar to that of the native gp41 six-helix bundle. We hypothesize that the α/β-peptide backbone in **10** may have an inherent reluctance to adopt the superhelical twist necessary for simultaneously engaging the entire NHR trimer binding surface. Additional experimental support for this idea comes from our recent work on homomeric α/β-peptide helix bundles, which showed that β-residue substitution is often accompanied by a decrease in superhelical twist relative to the helix bundle formed by the corresponding prototype α-peptide sequence (24, 26). Further understanding of the relationship between backbone composition and superhelical twist propensity will likely lead to foldamer CHR mimics with improved antiviral potency.

The results reported here represent a substantial advance relative to earlier efforts to develop unnatural oligomers that mimic α-helices involved in protein–protein recognition events (13, 14, 28, 41–46). Previous work has been limited to relatively short α-helical targets, typically only two to four helical turns. Efficacies of oligomers developed in these prior studies have generally been modest (IC_{50} values >1 μM). Moreover, in most previously studied systems, effective inhibition has been possible with small molecule antagonists. The present results are distinctive because we show that a long α-helix (~10 turns) can be structurally and functionally mimicked with a designed oligomer. To date, efforts to disrupt gp41 six-helix bundle assembly with small molecules have been relatively unsuccessful.

The present work demonstrates the value of designing unnatural oligomers that can "read" the recognition signals that have been evolutionarily encoded in natural proteins. Potent inhibition of HIV infectivity by α/β-peptides represents an important advance in the development of functional foldamers, but many challenges remain. It will be interesting to see whether this approach can be extended from α-helices to longer and more complex prototype sequences with defined tertiary folds. The success in mimicking the CHR α-helix of gp41 should inspire further exploration of sequence-based backbone modification for the creation of nonnatural oligomers that display protein-like recognition surfaces.

Materials and Methods

Peptide Synthesis. Detailed protocols for the synthesis and purification of **1**–**11** and CHR peptide modified at the N terminus with 5-carboxyfluoroscein (Flu-C38) can be found in the *SI Materials and Methods*.

Expression, Purification, and Refolding of gp41–5. Expression and purification of gp41–5 were carried out as previously described (15). The plasmid for gp41–5 was provided by Professor Stephen Harrison (Harvard University, Cambridge, MA). The full sequence of the construct used in this study, which differs slightly in the loop regions from the published sequence, is below.

MSGIVQQQNNLLRAIEAQQHLLQLTVWGIKQLQARILSGGSGGWMEWDRE-INNYTSLIHSLIEESQNQQEKNEQELLGGSGGSGIVQQQNNLLRAIEAQQHLLQ-LTVWGIKQLQARILSGGSGGWMEWDREINNYTSLIHSLIEESQNQQEKNEQELL-GGSGGSGIVQQQNNLLRAIEAQQHLLQLTVWGIKQLQARIL

Fluorescence Polarization Assays. The general experimental considerations for the FP assays, modified somewhat from the reported gp41–5 FP assay protocol, (15) were based on published methods (25). Briefly, the binding affinity of Flu-C38 for gp41–5 was measured by titrating gp41–5 against a 0.2 nM solution of labeled peptide. The K_d of the tracer was determined to be 0.4 ± 0.1 nM. Competition fluorescence polarization assays were carried out by 1:100 dilutions of inhibitor stocks in DMSO into a solution containing 2 nM gp41–5 and 1 nM Flu-C38.

Crystallization. Crystals were grown by hanging drop vapor diffusion. Diffraction data for the **1**+**3** and **1**+**8** complexes were collected on a Bruker X8 Proteum Diffractometer using Cu K_α radiation. Diffraction data for the crystals of **10** and the **1**+**10** complex were collected at the Life Sciences Collaborative Access Team beamline 21-ID-G at the Advanced Photon Source, Argonne National Laboratory. All structures were solved by molecular replacement. Detailed protocols for crystallization, data collection, data processing, structure solution and refinement can be found in the *SI Materials and Methods*.

Circular Dichroism Spectroscopy. Circular dichroism measurements were carried out on an Aviv 202SF Circular Dichroism Spectrophotometer. Spectra were recorded in a 2-mm cell with a step size of 1 nm and an averaging time of 5 s. Thermal melts were carried out in a 1-mm cell, monitoring at 222 nm, with 5 °C increments and an equilibration time of 10 min between each temperature change (a 20-min equilibration time gave similar results). Thermal unfolding data were fit to a simple two-state folding model using GraphPad Prism to obtain the reported $T_{m,app}$ values.

Antiviral Assays. A cell-to-cell-fusion assay based on the envelope glycoprotein of the HIV-1 clone HXB2 expressed in CHO cells and with U373-MAGI cells as targets was carried out as previously described (38). All of the α/β peptides showed no cytotoxicity at 5 μM, as judged by measuring the basal level of β-galactosidase expression in the U373-MAGI target cells. Inhibition of HIV-1 infectivity was measured on TZM-bl (JC53BL) cells, which express CD4, CXCR4, CCR5, and the luciferase gene under the control of HIV-1 long terminal repeat (LTR) (39). Viral stocks produced in PBMC of four HIV-1 strains were used: NL4–3, a clone derived from the X4-tropic T cell line-adapted isolate IIIB of clade B; HC4, an X4 primary isolate of clade B (47); and the two R5 primary isolates, CC 1/85 (clade B) (48) and DJ258 (clade A) (49). Briefly, TZM-bl cells were seeded the day before inoculation at a density of 10^5 cells per mL, 100 μL per well. Serially diluted peptide in 50 μL (or medium alone as a control) was added to each well. Then the virus, 40 $TCID_{50}$ in 50 μL, or medium only as a background control, was added to each well. On the third day, the wells were inspected by light microscopy. Wells with and without peptide were compared for cell confluency and morphology. No signs of toxicity were discerned at the highest concentrations of peptide used. The infectivity was then quantified in relative light units with the Bright-Glo Luciferase Assay System (Promega) according to the manufacturer's instructions. The experiment was performed three times. The signal of test wells was normalized to that of control wells without inhibitor after background subtraction from both. The percent inhibition of infectivity was expressed as a function of the $\log_{10}$ concentration of inhibitor in nM. A four-parameter sigmoid function was fitted to the data in Prism (GraphPad). The R^2 values for the fits were 0.95–1.0 for NL4–3; 0.98–1.0 for HC4; 0.95–0.98 for CC 1/85; and 0.92–0.98 for DJ258.

Protease Stability Assays. Assays were carried out as previously described (25). A detailed protocol can be found in *SI Materials and Methods*.

ACKNOWLEDGMENTS. We thank Dr. Gary Frey and Prof. Stephen Harrison for supplying a sample of the plasmid used for gp41–5 expression; Prof. James Keck and Prof. Katrina Forest for providing access to X-ray instrumentation; and PepTech for providing protected β^3-amino acids at a discounted price. This work was funded by the National Institutes of Health (GM56414 to S.H.G., CA119875 fellowship to W.S.H., AI42382 to M.L., and AI45463 and AI76982 to J.P.M.). L.M.J. was supported in part by the Chemistry-Biology Training Program (T32GM008505). Use of the Advanced Photon Source was supported by the U.S. Department of Energy, Office of Science, Office of Basic Energy Sciences, under Contract no. DE-AC02–06CH11357.

1. Arkin MR, Wells JA (2004) Small-molecule inhibitors of protein–protein interactions: Progressing towards the dream. *Nat Rev Drug Discov* 3:301–317.
2. Leader B, Baca QJ, Golan DE (2008) Protein therapeutics: A summary and pharmacological classification. *Nat Rev Drug Discov* 7:21–39.
3. Gallo SA, et al. (2003) The HIV Env-mediated fusion reaction. *Biochim Biophys Acta* 1614:36–50.
4. Chan DC, Fass D, Berger JM, Kim PS (1997) Core structure of gp41 from the HIV envelope glycoprotein. *Cell* 89:263–273.
5. Tan K, Liu J, Wang J, Shen S, Lu M (1997) Atomic structure of a thermostable subdomain of HIV-1 gp41. *Proc Natl Acad Sci USA* 94:12303–12308.
6. Weissenhorn W, Dessen A, Harrison SC, Skehel JJ, Wiley DC (1997) Atomic structure of the ectodomain from HIV-1 gp41. *Nature* 387:426–430.
7. Eckert DM, Kim PS (2001) Mechanisms of viral membrane fusion and its inhibition. *Annu Rev Biochem* 70:777–810.
8. Harrison SC (2005) Mechanism of membrane fusion by viral envelope proteins. *Adv Virus Res* 64:231–261.
9. Moore JP, Doms RW (2003) The entry of entry inhibitors: A fusion of science and medicine. *Proc Natl Acad Sci USA* 100:10598–10602.
10. Matthews T, et al. (2004) Enfuvirtide: The first therapy to inhibit the entry of HIV-1 into host CD4 lymphocytes. *Nat Rev Drug Discov* 3:215–225.
11. Eckert DM, Malashkevich VN, Hong LH, Carr PA, Kim PS (1999) Inhibiting HIV-1 entry: Discovery of D-peptide inhibitors that target the gp41 coiled-coil pocket. *Cell* 99:103–115.
12. Sia SK, Carr PA, Cochran AG, Malashkevich VN, Kim PS (2002) Short constrained peptides that inhibit HIV-1 entry. *Proc Natl Acad Sci USA* 99:14664–14669.
13. Ernst JT, et al. (2002) Design of a protein surface antagonist based on α-helix mimicry: Inhibition of gp41 assembly and viral fusion. *Angew Chem Int Ed* 41:278–281.
14. Stephens OM, et al. (2005) Inhibiting HIV fusion with a β-peptide foldamer. *J Am Chem Soc* 127:13126–13127.
15. Frey G, et al. (2006) Small molecules that bind the inner core of gp41 and inhibit HIV envelope-mediated fusion. *Proc Natl Acad Sci USA* 103:13938–13943.
16. Welch BD, VanDemark AP, Heroux A, Hill CP, Kay MS (2007) Potent D-peptide inhibitors of HIV-1 entry. *Proc Natl Acad Sci USA* 104:16828–16833.
17. Wang D, Lu M, Arora PS (2008) Inhibition of HIV-1 fusion by hydrogen-bond-surrogate-based α-helices. *Angew Chem Int Ed* 47:1879–1882.
18. Gellman SH (1998) Foldamers: A manifesto. *Acc Chem Res* 31:173–180.
19. Kirshenbaum K, Zuckermann RN, Dill KA (1999) Designing polymers that mimic biomolecules. *Curr Opin Struct Biol* 9:530–535.
20. Eschenmoser A (1999) Chemical etiology of nucleic acid structure. *Science* 284:2118–2124.
21. Hill DJ, Mio MJ, Prince RB, Hughes TS, Moore JS (2001) A field guide to foldamers. *Chem Rev* 101:3893–4011.
22. Goodman CM, Choi S, Shandler S, DeGrado WF (2007) Foldamers as versatile frameworks for the design and evolution of function. *Nat Chem Biol* 3:252–262.
23. Hecht S, Huc I, eds (2007) *Foldamers: Structure, Properties, and Applications* (Wiley-VCH, Weinheim, Germany).
24. Horne WS, Price JL, Keck JL, Gellman SH (2007) Helix bundle quaternary structure from α/β-peptide foldamers. *J Am Chem Soc* 129:4178–4180.
25. Horne WS, Boersma MD, Windsor MA, Gellman SH (2008) Sequence-based design of α/β-peptide foldamers that mimic BH3 domains. *Angew Chem Int Ed* 47:2853–2856.
26. Horne WS, Price JL, Gellman SH (2008) Interplay among side chain sequence, backbone composition, and residue rigidification in polypeptide folding and assembly. *Proc Natl Acad Sci USA* 105:9151–9156.
27. Dwyer JJ, et al. (2007) Design of helical, oligomeric HIV-1 fusion inhibitor peptides with potent activity against enfuvirtide-resistant virus. *Proc Natl Acad Sci USA* 104:12772–12777.
28. Sadowsky JD, et al. (2005) Chimeric ($\alpha/\beta+\alpha$)-peptide ligands for the BH3-recognition cleft of Bcl-x_L: Critical role of the molecular scaffold in protein surface recognition. *J Am Chem Soc* 127:11966–11968.
29. Chan DC, Chutkowski CT, Kim PS (1998) Evidence that a prominent cavity in the coiled coil of HIV type 1 gp41 is an attractive drug target. *Proc Natl Acad Sci USA* 95:15613–15617.
30. Ondetti MA, Engel SL (1975) Bradykinin analogs containing β-homoamino acids. *J Med Chem* 18:761–763.
31. Steer DL, Lew RA, Perlmutter P, Smith AI, Aguilar MI (2002) β-Amino acids: Versatile peptidomimetics. *Curr Med Chem* 9:811–822.
32. Sadowsky JD, Murray JK, Tomita Y, Gellman SH (2007) Exploration of backbone space in foldamers containing α- and β-amino acid residues: Developing protease-resistant oligomers that bind tightly to the BH3-recognition cleft of Bcl-x_L. *Chembiochem* 8:903–916.
33. Bryngelson JD, Wolynes PG (1987) Spin glasses and the statistical mechanics of protein folding. *Proc Natl Acad Sci USA* 84:7524–7528.
34. Cheng RP, DeGrado WF (2001) De novo design of a monomeric helical β-peptide stabilized by electrostatic interactions. *J Am Chem Soc* 123:5162–5163.
35. Appella DH, et al. (1997) Residue-based control of helix shape in β-peptide oligomers. *Nature* 387:381–384.
36. LePlae PR, Fisk JD, Porter EA, Weisblum B, Gellman SH (2002) Tolerance of acyclic residues in the β-peptide 12-helix: Access to diverse side-chain arrays for biological applications. *J Am Chem Soc* 124:6820–6821.
37. Schmitt MA, Choi SH, Guzei IA, Gellman SH (2005) Residue requirements for helical folding in short α/β-peptides: Crystallographic characterization of the 11-helix in an optimized sequence. *J Am Chem Soc* 127:13130–13131.
38. Deng YQ, Zheng Q, Ketas TJ, Moore JP, Lu M (2007) Protein design of a bacterially expressed HIV-1 gp41 fusion inhibitor. *Biochemistry* 46:4360–4369.
39. Wei XP, et al. (2002) Emergence of resistant human immunodeficiency virus type 1 in patients receiving fusion inhibitor (T-20) monotherapy. *Antimicrob Agents Chemother* 46:1896–1905.
40. Steger HK, Root MJ (2006) Kinetic dependence to HIV-1 entry inhibition. *J Biol Chem* 281:25813–25821.
41. Werder M, Hauser H, Abele S, Seebach D (1999) β-Peptides as inhibitors of small-intestinal cholesterol and fat absorption. *Helv Chim Acta* 82:1774–1783.
42. Kutzki O, et al. (2002) Development of a potent Bcl-x_L antagonist based on α-helix mimicry. *J Am Chem Soc* 124:11838–11839.
43. Kritzer JA, Lear JD, Hodsdon ME, Schepartz A (2004) Helical β-peptide inhibitors of the p53-hDM2 interaction. *J Am Chem Soc* 126:9468–9469.
44. Yin H, et al. (2005) Terphenyl-based helical mimetics that disrupt the p53/HDM2 interaction. *Angew Chem Int Ed* 44:2704–2707.
45. Yin H, Frederick KK, Liu DH, Wand AJ, DeGrado WF (2006) Arylamide derivatives as peptidomimetic inhibitors of calmodulin. *Org Lett* 8:223–225.
46. English EP, Chumanov RS, Gellman SH, Compton T (2006) Rational development of β-peptide inhibitors of human cytomegalovirus entry. *J Biol Chem* 281:2661–2667.
47. Trkola A, et al. (1998) Neutralization sensitivity of human immunodeficiency virus type 1 primary isolates to antibodies and CD4-based reagents is independent of coreceptor usage. *J Virol* 72:1876–1885.
48. Connor RI, Sheridan KE, Ceradini D, Choe S, Landau NR (1997) Change in coreceptor use correlates with disease progression in HIV-1-infected individuals. *J Exp Med* 185:621–628.
49. Louwagie J, et al. (1995) Genetic diversity of the envelope glycoprotein from human immunodeficiency virus type-1 isolates of African origin. *J Virol* 69:263–271.